PHILOSOPHICAL TRANSACTIONS OF THE ROYAL SOCIETY A MATHEMATICAL, PHYSICAL & ENGINEERING SCIENCES

The Effects of Strain on the Microstructures, Fabrics, and Deformation Mechanisms in Quartzites

S. White

Phil. Trans. R. Soc. Lond. A 1976 **283**, 69-86
doi: 10.1098/rsta.1976.0070

Phil. Trans. R. Soc. Lond. A. **283**, 69–86 (1976) [69]
Printed in Great Britain

The effects of strain on the microstructures, fabrics, and deformation mechanisms in quartzites

By S. White
Departments of Geology and Metallurgy, Royal School of Mines, Imperial College, London S.W.7

[Plates 2 and 3]

The *c*-axes fabrics and the intracrystalline microstructures of naturally deformed quartz indicate that dislocation deformation mechanisms are important natural deformation processes. Two mechanisms, dynamic recovery and cyclic dynamic recrystallization, can lead to steady state flow which is necessary if large strains are to be attained. Cold working followed by cataclasis can also produce a steady state flow, but is limited to low temperature, high stress environments.

Available data indicates that the *c*-axes preferred orientations and the optical strain features develop progressively as the strain increases. Recrystallization occurs by the continual rotation of sub-grains or by the development of small strain free grains. The new grains develop preferentially in the most misorientated areas of the deformed host grains, especially along deformation bands and in grain mantles. They have *c*-axes orientations similar to the range in orientation of the host grain in deformation bands and mantles.

Grain growth is inhibited if there is a rapid increase in the dislocation density in the new grains. Grain refinement then accompanies recrystallization and produces a quartz mylonite. The new grains may be subjected to further phases of deformation and grain refinement.

Deformation maps for quartz show that Coble creep replaces dislocation creep as the main deformation process when the grain size is less than 100 μm. The change is accompanied by strain softening and the maps imply that fine grained quartz mylonites are superplastic.

1. Introduction

Recent optical and transmission electron microscopy (t.e.m.) studies of both naturally and experimentally deformed quartz (McLaren & Retchford 1969; McLaren, Turner, Boland & Hobbs 1970; White 1971 *a*, 1973 *a*, *b*, 1975, 1976; McLaren & Hobbs 1972; Baeta & Ashbee 1973; Ardell, Christie & Tullis 1973; White & Treagus 1975) have established the importance of dislocation deformation mechanisms. They confirmed the validity of applying well established metallurgical principles to the study of natural deformation processes particularly in 'drier' environments, that is from mid-greenschist through to and including granulite facies conditions. These and other recent studies with a metallurgical bias (Wilson 1973; Bell & Etheridge 1973; Tullis, Christie & Griggs 1973; Lister 1974) have advanced our understanding of the development of quartz microstructures and *c*-axes fabrics during deformation.

However, a consideration of dynamic recrystallization as an integral part of the deformation has been largely neglected by geologists. Repeated recrystallization is known to occur during the hot working of metals and together with recovery has a softening effect that enhances the attainment of large ductile strains (Jonas, Sallars & Tegart 1969; Sah, Richardson & Sellars

1969, 1974; McQueen & Bergeson 1972; Stüwe & Ortner 1974). The first phase of recrystallization is initiated after a critical strain is reached. The newly formed grains are also subjected to deformation and may themselves subsequently recrystallize (Sah *et al.* 1969; Stüwe & Ortner 1974). A final unique grain size, which is dependent upon the applied stress and independent of the initial grain size (Sah *et al.* 1974) is produced. Do similar phenomena occur during the natural deformation of quartz and to what extent are the above data useful geologically? Furthermore, what is the effect of any grain refinement, produced by dynamic recrystallization, on the mechanism of deformation and on the rheological properties of quartz? These questions will be considered in this paper.

The progressive development of the intracrystalline microstructure and of the *c*-axes orientation of the constituent grains in a quartzite with increasing strain will be discussed first and this will be followed by a consideration of dynamic recrystallization and of the effect a change in grain size has upon deformation mechanism.

2. Dislocation deformation mechanisms capable of producing steady state flow

The attainment of large natural strains requires a deformation mechanism that can produce a steady state flow (see Heard, this volume). Dislocation mechanisms can produce such a flow if the internal strain energy in a grain associated with any increase in dislocation density and with dislocation entanglement, which combine to cause strain hardening, is continually reduced (discussed in White 1975*a*). This can be achieved in a wide range of materials by dynamic recovery, that is the thermally activated nonconservative motion of dislocations. They can then disentangle, annihilate each other and those remaining can be rearranged into low energy configurations such as sub-grain walls. Steady state deformation is established when the recovery rate balances the strain hardening rate. If deformation conditions, for example stress, changes then the recovery processes will try to re-establish steady state flow by slightly altering the arrangement of sub-grain walls. For example, more walls form if the stress increases and consequently the individual walls are more closely spaced; a dislocation then has a smaller distance to diffuse before reaching a wall and the recovery rate is effectively increased.

Recrystallization will be favoured if recovery cannot keep up with any increase in dislocation density. The internal strain energy is relieved by the formation of new strain free (dislocation free) grains. These in turn are deformed as the strain increases and may eventually recrystallize. This can give rise to cyclic hardening and softening and produces an overall steady state flow (Sah *et al.* 1969; Stüwe & Ortner 1974).

If diffusion is slow (low temperatures) and the increase in dislocation density is rapid (high stresses), then the internal intracrystalline stresses will increase rapidly and lead to rupturing. Subsequent deformation of a quartzite will be by cataclasis which can produce a steady state flow (Scholz 1968) and a possible strain softening (S. A. F. Murrell, personal communication). This is not, strictly, a dislocation process and will not be discussed in any detail.

Summarizing, the following processes which involve dislocations can lead to a steady state flow in materials:

(1) dynamic recovery,
(2) cyclic dynamic recrystallization,
(3) work hardening followed by cataclasis.

3. Development of microstructures

Intracrystalline microstructural development is most complete in quartz deformed in a recovery process and is least evident in the cataclasis process. However, as will be seen in later sections, most quartz grains undergo some recovery before recrystallization indicating that most steady state deformation is by a combination of dynamic recovery and dynamic recrystallization. Thus, the sequential development of microstructural features discussed in the following subsection holds for most naturally deformed quartz grains.

3.1. *Dynamic recovery*

The first observable effect of strain, even before any noticeable grain elongation, is the development of intracrystalline optical strain features. They are undulatory extinction, deformation bands and lamellae and sub-grains. Each of these features can be related to specific dislocation sub-structures which indicate that they develop during the initial strain increments (White 1973*a*, *b*, 1975; White & Treagus 1975) and will be summarized below.

Undulatory extinction can arise from two dislocation sub-structures. In some instances it can be related to large densities of individual dislocations which must contain more dislocations of one sign than the other. This causes the bending of the lattice and produces the undulatory extinction. More probably, it is the presence of lattice rotations due to the constraints imposed by neighbouring grains that cause the excess of dislocations of one sign. Thus the excess dislocations are geometrically necessary. They can be related to the lattice bending by the following equation (Cottrell P29, 1964),

$$R = 1/\rho b \tag{1}$$

where R is the radius of curvature of the bending, ρ, the number of excess dislocations (cm^{-2}), b, the Burgers vector of the dislocations and approximately 5×10^{-8} cm for quartz. A curvature of 1 cm would require an excess of 2×10^7 dislocations per square centimetre which is not a great number when it is considered that grains with well developed undulatory extinction may have observed densities of 10^9–10^{10} cm^{-2}.

The second, and more usual, cause of undulatory extinction are narrowly spaced dislocation walls, approximately along prism planes. Most of these walls have a similar sense of tilt and can form from the first type by recovery. The lattice rotation is preserved by a lower energy dislocation sub-structure.

Deformation bands also reflect dislocation sub-structures consisting of dislocation walls nearly parallel to prism planes and often containing segments parallel to a rhomb plane. The walls form elongated sub-grains which are concentrated into bands with most walls in a band having a similar sense of tilt. The area between bands is less deformed and contains more widely spaced walls which sometimes have an opposite sense of tilt. The internal bending in the grain is now concentrated into zones and is accommodated by fewer walls. Deformation bands with naturally deformed quartz are not simple polygonization features (Cahn 1950) as they develop both perpendicular to and parallel to the most active slip plane. Thus grains elongated in a [0001] direction in the foliation plane, indicating dominant prism slip, have deformation bands approximately parallel to the grain elongation and slip plane and probably represent slip bands. Whereas, if the grain is elongated with the [0001] direction normal to the foliation plane, indicating basal slip, the deformation bands are approximately perpendicular to the grain elongation (see Wilson 1975). A similar relation exists between the dominant slip plane and elongated sub-grains that form bands in crept materials (Feltham & Sinclair 1972).

Most deformation lamellae in naturally deformed quartz are zones of narrow sub-basal sub-grains and therefore are essentially deformation bands. However, in high stress environments they may be shear fractures or deformation twins which are decorated by a glass (White 1973*c*). Experimentally formed lamellae may be narrow zones of intense deformation marked by high dislocation densities (Hobbs, McLaren & Paterson 1972; Twiss 1974); zones of glass (Christie & Ardell 1974) or narrow sub-grains if produced during stress relaxation (McLaren *et al.* 1970). In all some seven structures have been correlated with deformation lamellae. It is difficult to distinguish between each with an optical microscope as all types are often imaged as small phase objects (McLaren *et al.* 1970).

Both the elongate and the equidimensional sub-grains that are seen with an optical microscope can be correlated to large sub-grains in electron micrographs. They are misorientated from each other by more than 1° and contain within them a mosaic of smaller, less misorientated (less than 1°) sub-grains which constitute a sub-grain in sub-grain structure. The size of the small sub-grains, and to some extent the large sub-grains should be inversely proportional to the stress but independent of strain. Thus sub-grains in a wide range of mylonites have similar sizes and are smaller than those in normal quartzites (White 1976). The lattice bending is now accommodated by a single wall which has replaced a group of walls.

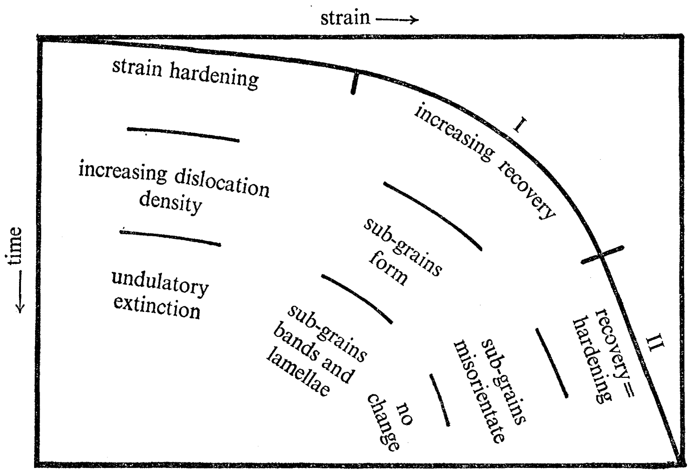

FIGURE 1. Progressive development of optical strain features in deformed quartz grains with an increase in intracrystalline strain, as shown by grain elongation. (Taken from White 1975.)

All of the sub-grains, including those forming deformation bands and lamellae contain appreciable densities of unbound dislocations (typically between 10^7 and 10^8 cm^{-2}) and dislocation loops.

The dislocation sub-structures described above, except for the high densities of dislocations causing undulatory extinction, are similar to those produced by recovery during creep (discussed by White 1975) and because of this he postulated that they should develop in the same sequence as that observed for crept materials. The proposed sequence is shown in figure 1, and shows that the dislocation structures evolve towards the one with the lowest energy and capable of accommodating the imposed lattice rotations. Steady state deformation follows the development of a stable sub-grain structure. Thus the optical strain features develop in the initial stages of deformation and remain constant apart from a progressive increase in sub-grain misorientation, especially the large sub-grains, during steady state flow. The sub-grain structures, and their related optical strain features, are extremely stable because they are constructed from low energy dislocation arrangements which contain geometrically necessary dislocations and therefore are not annealed out during uplift.

The dislocation sub-structures are seldom developed homogeneously throughout a grain. It was noted above that deformation bands are zones of more intense lattice misorientation and represent an inhomogeneous distribution of sub-grains. Apart from this there is often a detectable difference in the optical strain features and dislocation sub-structures between grain edges and the central areas of grains. The change may be slight, for example a decrease in sub-grain size and an increase in misorientation near the grain margins or may be more dramatic as recorded by White (1973*b*) and summarized in figure 2. In the grains he described, the central areas contained deformation bands and lamellae while the edges consisted of small,

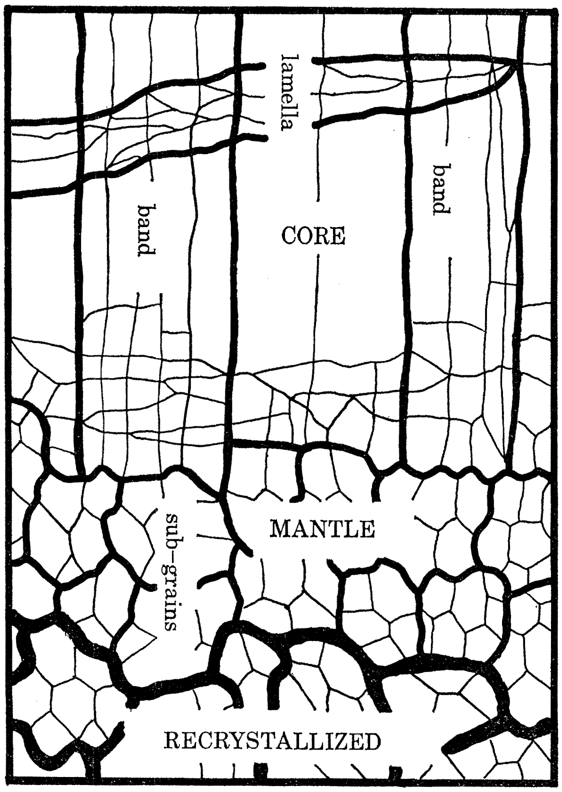

FIGURE 2. A sketch of a typical core and mantle structure as seen in electron and optical micrographs and discussed by White (1973*b*). New grains develop in the edge of the mantle by the increasing misorientation of clusters of sub-grains. The heavy lines mark grain boundaries, medium lines the extent of optical strain features, and the light lines the individual sub-grains seen in electron micrographs. The small equidimensional sub-grains have diameters of around 5 μm.

highly misorientated, sub-grains which contained smaller sub-grains. Gifkins (1975) has referred to this as a core and mantle structure; the core being the less deformed central area of a grain and the mantle being the marginal zone. He suggested that a core behaves as an isolated single crystal while the mantle absorbs the strain gradient between the adjacent cores, that is the deformation is concentrated in the mantles with a strain gradient between core and mantle.

Recrystallization can occur during dynamic recovery. The sub-grains continually increase their misorientation as the strain increases. The misorientation, θ, across a sub-grain boundary is approximately (Hull P182, 1965)

$$2 \sin \tfrac{1}{2}\theta = b/h, \tag{2}$$

where b is the Burgers vector of the dislocations, and h is the spacing between dislocations. More dislocation will enter a boundary, thereby decreasing h, as the strain increases and cause an increase in misorientation. The limit is reached when dislocations are so closely spaced that they lose their individual identity and when this happens the boundary is no longer a low angle sub-grain boundary but a high angle, mobile, grain boundary. If a spacing of 2.5 nm (five lattice spacings) is taken as the minimum distance before core interference (Hull, P182, 1965) then a low angle boundary becomes a grain boundary when the misorientation is about 10°. A sub-grain then becomes a small grain and can be recognized as such in petrographic thin sections. The new grains studied by White (1973*b*) contained smaller less misorientated grains when studied by t.e.m. The recrystallization mechanism just described is an integral part of the dynamic recovery sequence and has been observed in experimentally deformed (Hobbs 1968) as well as naturally deformed quartz grains.

The new grains will preferentially develop in the most deformed and misorientated areas such as along deformation bands and in grain mantles. They have a crystallographic orientation similar to the old grains. Recent studies of the Mt Isa mylonites indicate that the misorientated regions of individual old grains are related by a rotation about an *a*-axis and that the new grains are related to the old by a similar rotation (McLaren & Hobbs 1972; White & Wilson, in preparation).

3.2. *Dynamic recrystallization*

Dynamic recrystallization occurs when recovery cannot keep pace with strain hardening and the old grains are gradually consumed by strain free new grains. Recrystallization will occur after small strains if little or no recovery occurs or, if the recovery and strain hardening rates are almost equal deformation bands, lamellae and sub-grains will develop (figure 3*a*, *b*, plate 2) and recrystallization will not be initiated until much larger strains have been reached. Again, as in the recovery process, the new grains develop preferentially along deformation bands and in grain mantles as it is in these regions that the lattice becomes sufficiently misorientated for the development of a stable high angle boundary (Doherty 1974) which can bulge to form viable new grain nuclei. In some instances the new grains are formed from bulges developed during strain induced grain boundary migration (Hutchinson 1974) of an existing boundary into its less deformed neighbouring grain (figure 3*c*). This requires a strain gradient between adjacent grains and is unlikely to operate once all grains have a well developed mantle and may be restricted to recrystallization after low strains.

The new grains, irrespective of their mode of nucleation, become deformed, develop optical strain features and may undergo further recrystallization. In some circumstances the host grains are immediately replaced by small, approximately 5 μm diameter, grains whereas in others there is a progressive decrease in grain size with increasing strain (J. Carreras, personal communication). Once again, the small grains are sometimes clustered into groups, each group

---

Description of plate 2

Figure 3. (*a*) An optical micrograph (crossed nicols) of new grains, on the left, developing at the edge of a quartz grain containing deformation bands, from quartz mylonites along the Outer Hebrides Thrust at Scalpay.

(*b*) An electron micrograph showing a new grain growing into a deformed quartz grain. The sub-grain walls, arrowed, form a deformation band. Note the dislocations in the new grain.

(*c*) An optical micrograph (crossed nicols) showing a new grain, *n*, formed from a grain boundary bulge.

Figure 6. Fibrous quartz overgrowths on a magnetite grain in the Mt Isa quartz mylonites. Note the fine grain size of the matrix.

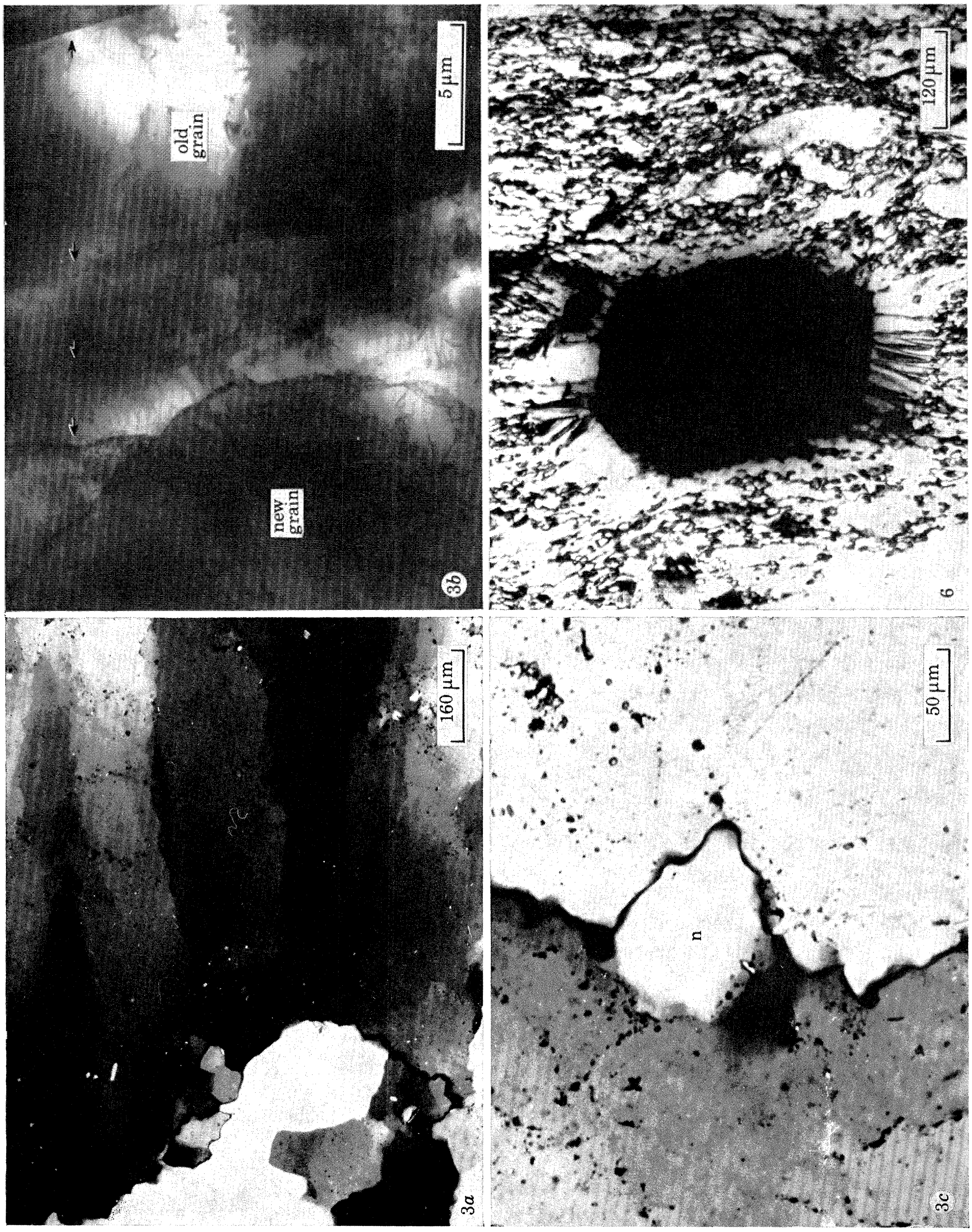

FIGURES 3 AND 6. For description see opposite.

(*Facing p.* 74)

PHILOSOPHICAL TRANSACTIONS OF THE ROYAL SOCIETY A MATHEMATICAL, PHYSICAL & ENGINEERING SCIENCES

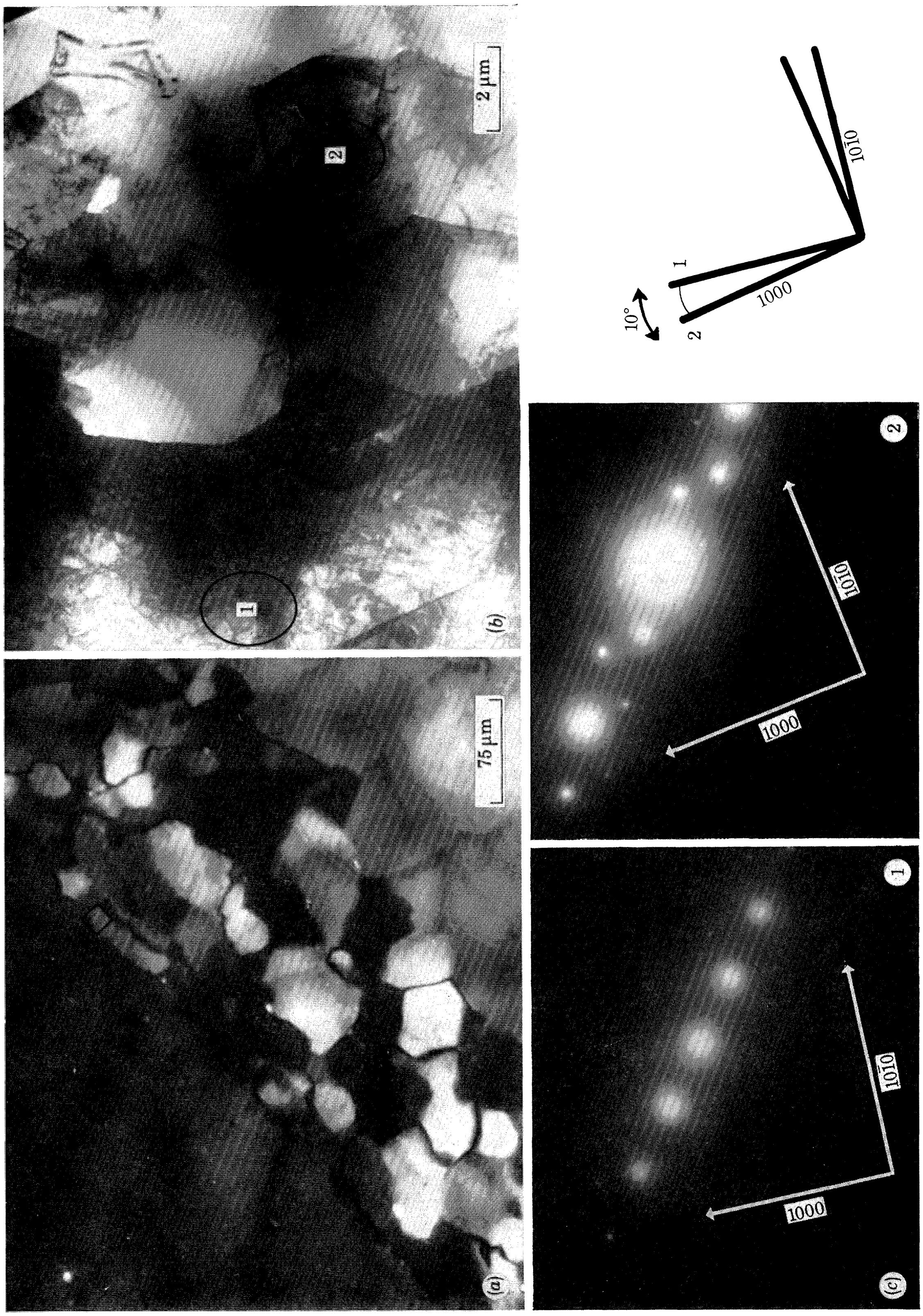

Figure 4. For description see opposite.

appearing as a single grain in the optical microscope (figure 4*a*, *b*, plate 3). The formation and cause of the clustering is under investigation. The AVA diagrams of Phillips (1965) suggest that it can occur on all scales. The ultimate grain size produced by sequential dynamic recrystallization requires further investigation, but metallurgical data (Sah *et al.* 1974) suggests that it may be controlled by the magnitude of the stress.

The orientation of the new grains and their crystallographic relationship to the host grains can be determined from selected area diffraction patterns obtained in the electron microscope. A study has been made of new to old grain relationships in partially recrystallized quartz in a mylonite pod in cataclasites associated with the Outer Hebrides Thrust at Pabbay. Most old grains exhibit little evidence of recovery and only have a marked undulatory extinction. Some grains contain deformation bands. Recrystallization has occurred in all grain mantles and along some deformation bands (figure 4*a*, *b*). The misorientation in the old grains increases in the mantles and as deformation bands are approached and is a rotation about an *a*-axis (figure 4*c*). Similar rotations have been reported in many deformed quartz grains (Bailey, Bell & Peng 1958; Phillips 1965). The majority of the new grains were related by a rotation of between 1 and 25° about an *a*-axis to their host grain (figure 5) and will be referred to subsequently as type I new grains. The above spread is within the range commonly found across deformation bands in quartz (Phillips 1965; Carreras 1974). Phillips also recorded that most of the newly formed grains in his specimens were misorientated by less than 22° from the old grains. Hobbs (1968) in an experimental deformation study reported a close similarity between the orientation of the new grains and host grain within the deformation bands along which the new grains had developed. Thus the misorientation of the host grain in the mantles and bands may have a controlling influence on the orientation of the new grains in quartz. Similar new grain to old grain relationships are found in metals (Cahn 1974).

Some of the grains in figure 5 plot well outside the spread of the type I grains and will be designated type II new grains. The reason for the two different orientations which may be important in grain growth (see next section) is not known.

3.3. *Work hardening followed by cataclasis*

Undulatory extinction is the only expected optical strain feature. Thus the final microstructure should be that of a cataclasite with porphyroclasts containing undulatory extinction. However, the high densities of dislocations may be rearranged into lower energy configurations during post tectonic annealing, although this does not always seem to happen (White 1975*b*). Rigid particle rotation during cataclasis precludes any unique crystallographic relationship between the old grains and the fragments and suggests that the quartz fragments should be randomly orientated.

Description of plate 3

Figure 4. (*a*) An optical micrograph (crossed nicols) of recrystallized grains along a deformation band in a quartz grain from a quartz mylonite associated with the Outer Hebrides Thrust at Pabbay. The section has been thinned for electron microscopy and the mottling effect is a surface artefact produced during ion thinning.

(*b*) An electron micrograph covering approximately the area within the rectangle in (*a*) and showing the contact between old grain, on the left, and new grains. Note the apparent difference in new grain size when compared with (*a*).

(*c*) Selected area diffraction patterns covering the areas marked 1 and 2 in (*b*). The 0001 and $10\bar{1}0$ plane normals are marked on both patterns. Both sections are in the $(1\bar{2}10)$ plane and 2 is rotated clockwise through approximately 10° from 1 about an *a*-axis.

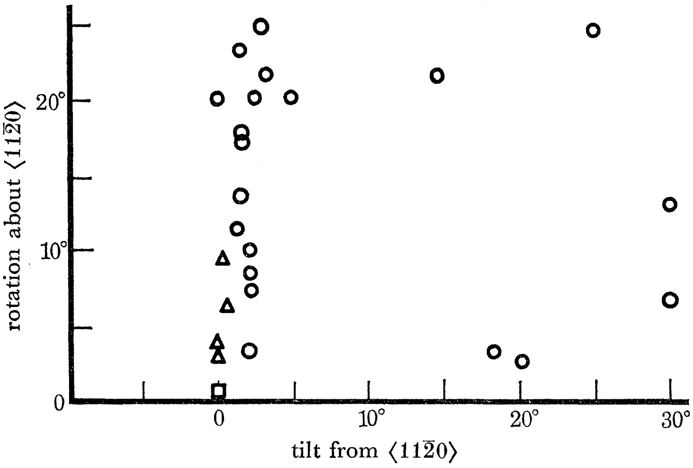

FIGURE 5. The crystallographic relation between the old grain and the new grains shown in figure 4. The estimated accuracy of each point is ± 3°. □, old grain centre; △, old grain edge; ○, new grains.

4. Microstructural changes after recrystallization

The formation of new grains and their coalescence to form a completely recrystallized matrix is termed primary recrystallization and is normally followed by grain growth, secondary recrystallization (Honeycombe P331, 1968). The driving force for primary recrystallization is the reduction in strain energy achieved by strain induced grain boundary migration and, to a lesser extent, the reduction in grain boundary energy. The latter is the sole driving force for secondary recrystallization. In both cases, all else being equal, those boundaries with the greatest misorientation will tend to grow the fastest. Metallurgical evidence (Gordon & Vandermeer 1966) indicates that the rate of movement of the boundaries increases rapidly with misorientations up to 25° and less rapidly for higher misorientations. A normal coarse grained quartzite results and, as it is being continuously deformed, its constituent grains will exhibit optical strain features. Grain growth should be inhibited once all the grains have a well developed core and mantle structure.

Grain growth will be inhibited if the stress is sufficient to cause a rapid increase in the dislocation densities in the newly formed grains (Sah *et al.* 1974). Recrystallization then produces grain refinement and it is in such circumstances that quartz mylonites can develop. Although the ultimate grain size of a mylonite may be stress dependent, the actual grain size may reflect the strain especially if each phase of recrystallization is accompanied by grain refinement. However, if the ultimate grain size is established during the first recrystallization phase, then the grain size of a mylonite will be independent of strain and inversely proportional to the flow stress. A stress gradient across a mylonite zone will be reflected in a progressive decrease in the grain size of the mylonite.

5. Fabric development

An understanding of the genesis of quartz *c*-axes fabrics has not been the most successful branch of structural petrology. Until recently, most accepted interpretations have been based on non-hydrostatic thermodynamics (see Paterson 1973). However, the predicted *c*-axes fabrics did not include the most commonly observed preferred orientations. The reason for this, as Paterson pointed out, is that the above thermodynamic treatment is invalid if deformation has been by dislocation processes. The ubiquity of optical strain features in the grains of deformed quartzites is an indication of the importance of dislocation glide mechanisms and suggests that fabric development ought to be considered in this light.

In a polycrystalline aggregate in which deformation is constrained, the operation of a dominant single slip plane in a given grain will result in a tendency for that grain to rotate into an orientation with zero resolved shear stress along the slip plane. In reality, the situation is more complicated because of the simultaneous operation of several slip systems. This is taken into account in theoretical treatments of preferred orientation development such as the Taylor–Bishop–Hill theory or the less rigorous Calnan–Clewes theory (Dillamore & Roberts 1965; Chin 1969; Dillamore & Katoh 1971). Both theories have been used to predict quartz *c*-axes fabrics (Bhattacharya & Pasayat 1968; Tullis *et al.* 1973; Lister 1974). Lister simulated all of the commonly observed *c*-axes fabrics. He also demonstrated the important effect that deformation path has upon fabric development. The dominant slip systems in quartz are temperature and stress dependent (Baeta & Ashbee 1970; Carter 1971; Ave'Lallement & Carter 1971). Low temperature and, or, high stresses favour dominant basal slip in an *a*-direction whereas higher temperatures, low stresses and a high lattice water content favour prism slip in an *a*-direction or slip on a second order prism in a *c*-direction at still higher temperatures. The basal slip will produce a maximum of *c*-axes perpendicular to the foliation and lineation whereas the prism slip will concentrate the *c*-axes in the plane of the foliation and if slip in a single *a*-direction dominates then the maximum concentration will be approximately perpendicular to the lineation. This last fabric is an end member of two groups of *c*-axes fabric patterns normally referred to as crossed girdles (Phillips 1945; Sylvester & Christie 1968) and as *b–c* girdles (Balk 1952; Bhattacharya & Pasayat 1968) and suggests that both types differ only in the relative amounts of subsidiary basal and rhomb slip. Wilson (1975) recently observed that the temperature of deformation was reflected in the *c*-axes fabrics of some ribbon quartz mylonites and found that the fabrics corresponded to the preferred orientations that were expected from a change in slip with a change in temperature. A similar effect of temperature, and possibly of stress, was recorded, but not explained, by Phillips (1945) who observed that the quartz grains in the Moine schists away from the Moine thrust (deformed during amphibolite grade conditions) had crossed girdles but those deformed in the Moine thrust zone (greenschist facies conditions) had *c*-axes maxima perpendicular to both foliation and lineation.

The Taylor–Bishop–Hill theory also predicts that the referred orientation of the quartz *c*-axes should become more intense, that is approach that theoretically predicted, with increasing strain. Hara *et al.* (1973) found that such a relation existed in shear zones and a similar relation can be seen on a regional scale (Balk 1952; Sylvester & Christie 1968; Marjoribanks 1974). However, the effect of strain was recorded some time ago by Fellows (1943) and by Phillips (1945) who noted that the intensity of the *c*-axes fabrics in regionally deformed quartzites increased as the intensity of deformation increased.

The crystallographic relation between old and new grains in recrystallized quartzites, as discussed in the previous section, indicates that there should not be a great change in *c*-axes fabric patterns upon recrystallization; with the degree of preferred orientation of the new grains dependent mainly upon the strain prior to recrystallization. The new grains should have similar but more diffuse patterns. This is exactly what is found and, to the writer's knowledge, was first recorded by Phillips (1945) in his study of the Moine schists. He recorded that 'selective diagrams of larger relict grains and of smaller recrystallized grains, in every instance so far examined, show concordant girdles but the girdle of recrystalized grains is in comparison less well defined' and concluded his study by stressing 'the readiness with which quartz suffers recrystallization and the reluctance which it shows to undergo reorientation'. A similar relation between old and new grains has been recorded for quartz from a number of localities and environments (Ransom 1971; Wilson 1973; Carreras 1974) and also in experimentally deformed and recrystallized single crystals (Hobbs 1968).

The angular relation between old and new grains may alter as a result of grain growth. It can be argued, by considering a two stage grain growth process, that the patterns will first become more diffuse and then alter radically. The majority of small newly formed grains have *c*-axes orientations close to that of their parent grains (see §3.2). However, both Phillips (1965) and Hobbs (1968) found that grains with misorientations greater than 20° grew fastest and these would include the most misorientated of type I and all type II new grains on figure 5.

The elimination of the remainder of type I grains should increase the diffuseness of the *c*-axes fabric patterns and is a possible explanation for the large (20–50°) old grain–new grain misorientations recorded by Ransom (1971) and Wilson (1973) without a fundamental change in *c*-axes patterns. However, during exaggerated (second stage) grain growth the most misorientated of all new grains, that is the most misorientated type II new grains, cannibalize all remaining grains and should form a new pattern based on elements of the old pattern and which because of the preferential growth of a few grains will be much sharper than the previous pattern. The development of a new pattern during exaggerated grain growth has been reported by Wilson (1973).

Further dislocation deformation after dynamic recrystallization will inhibit grain growth and will also sharpen the preferred orientation of the new grains. This has been found in the Cabo de Creus mylonites by Carreras (1974). However, if the grains continue to rotate in a dynamic recovery deformation or if there is a change in deformation mechanism to one involving grain boundary sliding and rotation, then the fabrics will become increasingly diffuse but without a fundamental change in pattern.

Finally, summarizing this section, there is evidence in the recent and in the older literature that many quartz *c*-axes fabrics develop by dislocation processes and that the fabrics can be predicted by the Taylor–Bishop–Hill theory. A given *c*-axes fabric depends upon deformation conditions and progressively develops with increasing strain. It is not greatly altered during dynamic recrystallization but may be subsequently altered by exaggerated grain growth, grain boundary sliding and rotation or a change in deformation conditions. There is no reason why quartz fabric studies should not play a vital role in the study of natural deformation processes.

6. Change in deformation mechanism accompanying a reduction in grain size

Two features associated with mylonites, irrespective of their mineralogy, have attracted attention. They are, the concentration of large strains within narrow mylonite zones and the presence of overgrowths, fibrous pressure shadows and fibrous infillings in broken porphyroclasts in many mylonites (Fairbairn 1950; Sutton & Watson 1959; Johnston 1961; Cloos Pl. 60, 1971). The microstructural features are indicative of diffusion or solution transport and in many instances are undoubtedly synchronous with neo-mineralization. But then at what stage in mylonitization does neo-mineralization occur? Pressure shadows (figure 6, plate 2) and styolites can be seen in quartz mylonites and do not appear to be definitely related to neomineralization in all cases. Both are common in the finest grained areas of the Mt Isa mylonites (C. J. L. Wilson, personal communication) especially where the grain size is less than 20 μm but are not present in the Cabo de Creus mylonites (Carreras 1974) which also formed under greenschist conditions but which have a grain size of 100 μm.

Both of the above features can be explained if there is a change in deformation mechanism from dislocation creep to diffusion creep with an accompanying strain softening. Furthermore the narrowness of mylonite zones is a further indication that the required grain refinement occurred during dislocation creep. If they formed by a dislocation glide process then the Hall–Petch relation (Honeycombe P234, 1968) namely

$$\sigma_f = \sigma_i + kd^{-0.5}, \tag{3}$$

where σ_f is the flow stress, σ_i the internal or friction stress, k, a constant and d, the grain diameter, would apply and the resistance of a mylonite to further flow would increase as the grain size decreased. This would induce rapid lateral migration of a mylonite zone for which there is no field evidence Although dislocation creep processes are required to produce the recrystallization needed for grain refinement, they result in a strain rate which is independent of grain size and they cannot give the degree of strain softening required to preferentially concentrate deformation to the smallest grain size zone. However, strain rate is inversely proportional to grain size if deformation is by diffusion creep and for this to become dominant would require a change in deformation mechanism with grain refinement.

The effect of progressively reducing grain size on the operative deformation mechanism and in turn on the strain rate for constant stress and temperature can be shown in deformation maps of the type developed by Ashby (1972) and recently applied to the mantle deformation of olivine by Stocker & Ashby (1973). They are constructed by equating the constitutive strain rate equations for deformation by dislocation glide, dislocation creep and diffusion creep mechanisms and determining which mechanism results in the highest strain rate for given deformation conditions, namely stress, temperature and grain size. The field over which a given mechanism dominates can then be plotted. As stated previously, there is no evidence to suggest that dislocation glide will permit large strains before cataclasis which will then produce narrow zones of cataclasites rather than of mylonites. Thus only dislocation creep and diffusion creep will be considered in this contribution. A glide field has been included in the quartz maps produced by Rutter (this volume) and lies outside the conditions likely to be attained in the crust. Stocker & Ashby (1973) reached a similar conclusion for the glide deformation of olivine.

The steady state creep strain rate of many materials obey similar constitutive equations (Ashby 1972; Kirby & Raleigh 1973; Stocker & Ashby 1973; Mohamed & Langdon 1974; Gifkins 1975; Heard, this volume).

They are:

for dislocation creep
$$\dot{\epsilon} = \frac{AD_v Gb}{kT}\left(\frac{\sigma}{G}\right)^n, \tag{4}$$

and for diffusion creep
$$\dot{\epsilon} = \frac{21 D_v V}{kTd^2}\left(1+\frac{\pi\delta D_b}{dD_v}\right), \tag{5}$$

where A is a dimensionless constant called the Dorn parameter, D_v the volume (or lattice) diffusivity, D_b the grain boundary diffusivity, b the Burgers vector, σ the differential stress,

G the temperature compensated shear modulus, T the deformation temperature in degrees absolute, n a dimensionless constant, k the Boltzman constant, V the activation volume (22 cm^3/mol), d the grain diameter, and δ the grain boundary width ($= 2b$).

If in equation (5), $(\pi\delta/d)\ (D_b/D_v)$ is less than 1 then deformation is by stress induced lattice diffusion (Nabarro-Herring creep) or if this term is greater than 1 deformation is by stress induced grain boundary diffusion (Coble creep).

Either differential or deviatoric stress can be used in equations 4 and 5 and one can be substituted for the other as long as the corresponding multiplying factor is incorporated into the equations (see Nye 1953). There is some disagreement (Mohamed & Langdon 1974; Gifkins 1975) about the value of the numerical constant in equation (5) but the differences are not sufficient to radically affect the position of the deformation fields.

Creep data for quartz, in common with most minerals, is scanty. Diffusion data is particularly needed. Tullis *et al.* (1973) experimentally produced quartz mylonites which had microstructures, as seen in both the optical and transmission electron microscopes, and *c*-axes fabrics identical to their natural equivalents. They were formed at 900 °C, at a differential stress of about 100 MPa (1 kbar) and a strain rate of $10^{-7}\ s^{-1}$; higher strain rates and lower temperatures produced work hardening requiring high stresses to obtain moderate strains. Thus, a limit of 100 MPa may be taken as the highest differential stress permissible before glide dominates. The experimental values of Tullis *et al.* can be extrapolated to the lower temperatures and strain rates likely to be of significance during crustal deformation if the value of D_v is known at the temperature under consideration. This can be calculated for 900 °C from the above work by substituting in equation (4) and determined at various temperatures by the Arrenhuis relation.

$$D_{v(T)} = D_0 \exp\left(-Q_v/RT\right), \tag{6}$$

where D_0 is the absolute diffusivity, R the gas constant, and Q_v the activation energy for volume diffusion. However, the Dorn parameter in equation (4) must be determined first. It can be calculated if the value of n is known (Stocker & Ashby 1973). A value of 4 was used (see Rutter, this volume).

Recovery in quartz is dependent upon ion diffusion especially the movement of proton and hydroxyl ions. Grain boundary water had caused 'water' weakening during the experiments under consideration (Ardell *et al.* 1973) and naturally deformed quartzites are expected to be in a 'water' or impurity ion weakened condition. The activation energy for impurity ion diffusion in quartz ranges from 63 kJ $mole^{-1}$ (15 kcal mol^{-1}) for OH^- diffusion (White 1971*b*) to 105 kJ mol^{-1} (25 kcal mol^{-1}) for Na^+ ions (Frischat 1970). Proton diffusion has a value of about 84 kJ mol^{-1} (20 kcal mol^{-1}) (Kats 1962). An average value of 84 kJ mol^{-1} was used for Q_v. The value of D_0 calculated from the results of Tullis *et al.* is $5 \times 10^{-14}\ cm^2\ s^{-1}$ and this was also used in diffusion creep calculations (discussed in detail in Stocker & Ashby 1973). The strain rates for dislocation creep at various stresses and temperatures can now be calculated. The diffusion fields were plotted using the same data as used by Rutter except for taking $Q_b = \frac{1}{2}Q_v$ as suggested by Gifkins (1975) rather than the $\frac{2}{3}Q_v$ used by Stocker & Ashby. The lower value of Q_b will place a slightly greater emphasis on Coble creep (compare figure 7*b* with Fig. 7 in Rutter) and this will help compensate for the slightly higher strain rates expected from grain boundary sliding which Ashby (1972) includes in Coble creep and also from the enhancement of grain boundary diffusion rates by the presence of water in the grain boundaries of quartzites. In other words, grain boundary sliding and water assisted diffusion and transport processes

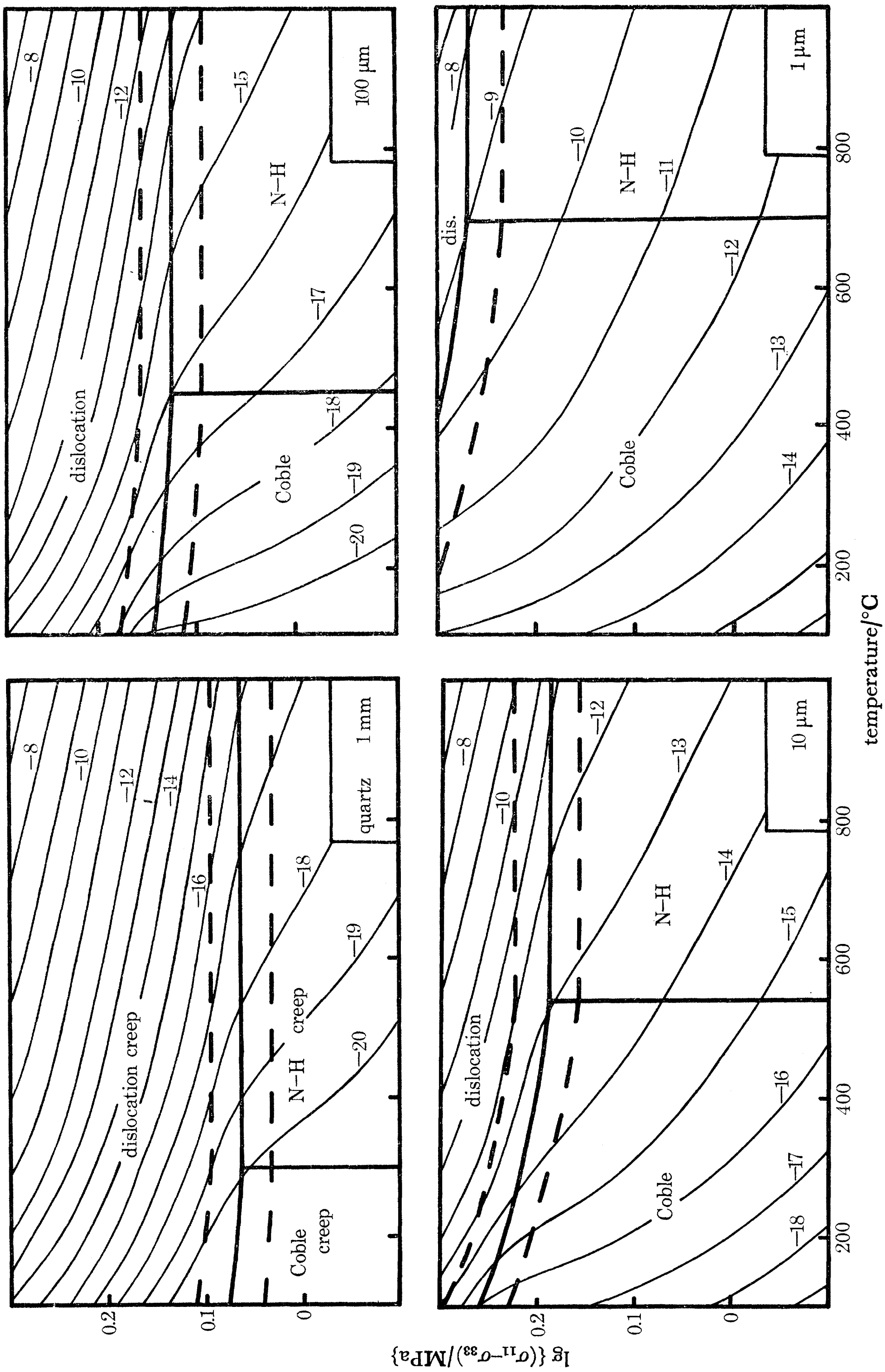

FIGURE 7. Deformation mechanism maps for quartz of differing grain size. Strain rate contours, $\lg_{10}\ s^{-1}$, are shown. The values of $\sigma_{11}-\sigma_{33}$ are based on values of the shear modulus at 900 °C (see Rutter, this volume).

(pressure solution) have been included under Coble creep. The author can find no evidence to suggest that large amounts of water are involved in mylonite formation. The small increase in the water content of mylonites, as indicated by retrogressive metamorphic mineral assemblages will aid grain boundary diffusion processes and should increase the Coble creep strain rate. Furthermore, pressure solution processes explain neither the progressive grain refinement with increasing strain in mylonite zones nor the similarity in the *c*-axes fabrics of the new and old grains. Pressure solution does not account for the optical strain features, dislocation substructures and *c*-axes fabrics so common in all naturally deformed quartzites and it is suggested that it may not be a significant deformation mechanism for relatively pure quartzites. A separate pressure solution field has not been considered for these reasons.

Deformation maps for grain sizes from 1 mm to 1 μm are presented in figure 7. The grain sizes in the maps refer to the mean grain size of a quartzite or of the pervasive matrix in a quartz mylonite. Strain rate contours have been included and the strain rate and deformation mechanism operative at a given grain size, stress and temperature can be read off. The boundaries between fields mark the positions where two processes produce equal strain rates. The broken line on either side of the dislocation creep and diffusion creep boundary mark overlaps of one order of magnitude in strain rate. Both types of deformation processes are expected to operate in these zones. The coexistence of Coble and Nabarro–Herring creep can be seen by a change in slope of the strain rate contours as they pass from the one field to the other and indicate a wide overlap zone.

The assumptions made in the construction of the maps and especially the lack of accurate diffusion data preclude these maps having other than 'ball-park' accuracy. However, they do show that the diffusion creep field expands at the expense of dislocation creep with a reduction in grain size and indicate that Coble creep will be the main deformation mechanism under crustal conditions for quartzites with a grain size of 10 μm or less. The maps also show that strain softening occurs with the onset of diffusion creep. Thus for a constant stress of 10 MPa and a temperature of 400 °C, a quartzite with a grain size of 1 mm will deform at a strain rate of about $10^{-14}\ s^{-1}$, and this increases to $5 \times 10^{-14}\ s^{-1}$ and to $10^{-11}\ s^{-1}$ for grain sizes of 10 and 1 μm respectively.

The maps are not grossly inaccurate as they bear out many field observations. They predict that dislocation creep mechanisms are the most important deformation process for quartzites with a grain size greater than 100 μm. This prediction is supported by the ubiquity of optical strain features and the presence of *c*-axes fabrics reflecting dislocation deformation in naturally deformed quartzites. They also predict a change in deformation mechanism for grain sizes much less than 100 μm and that fine grained quartz mylonites will deform, under similar conditions, much faster than coarse grained mylonites or quartzites. The maps imply that fine grained mylonites deformed by Coble creep may be effectively superplastic (Ashby & Verrall 1973).

The accuracy of the maps will be improved as more experimental and field observations become available and there is no reason why they should not be extended to polymineralic rocks once experimental data becomes available.

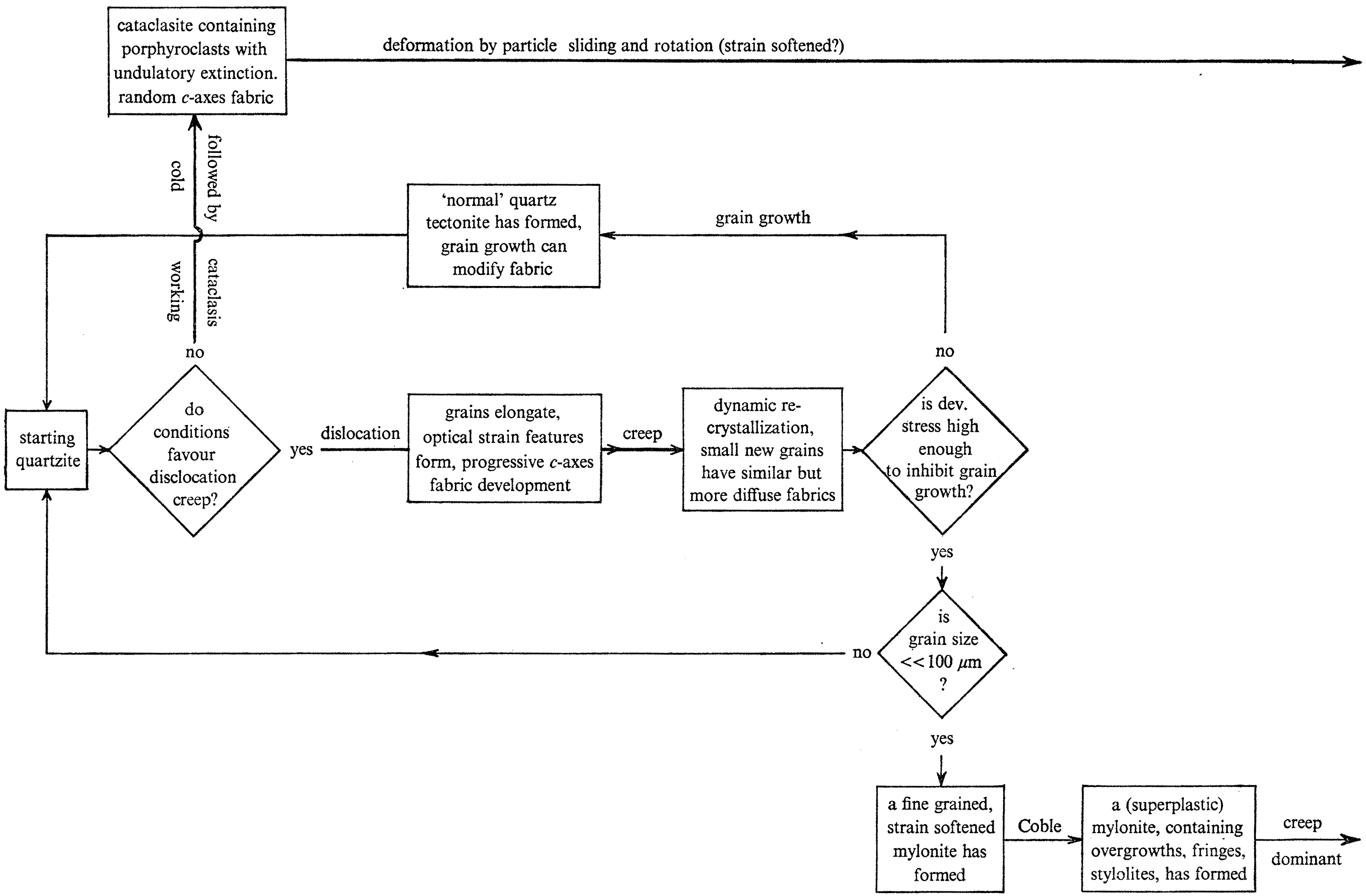

FIGURE 8. A simplified flow chart summarizing the progressive deformation of and texture and fabric development in quartzites.

7. Summary

Both ductile and cataclastic processes can produce a steady state flow which is required for the attainment of large natural strains in quartzites. Cataclastic processes which precede cold working of the quartzites, are favoured by low temperatures and high stresses and can lead to strain softening. The quartz porphyroclasts and fragments should not have any preferred crystallographic orientation because of the dominance of rigid particle rotation.

The microstructures and textures of naturally deformed pure quartzites indicate that most quartz is ductile during a natural deformation and that dislocation mechanisms account for the ductility. Two dislocation mechanisms can produce a steady state flow; they are dynamic recovery and dynamic recrystallization, with most quartzites deforming by a combination of both mechanisms. The optical strain features – undulatory extinction, deformation bands and lamellae and sub-grains – form during the initial strain increments. Their development in a grain is often heterogeneous and leads to the formation of a core and mantle structure. A preferred orientation of the *c*-axes of the quartz grains develops as the strain increases, with the actual fabric pattern dependent on the operative slip systems which in turn depend on temperature, stress and lattice 'water' content.

Recrystallization occurs in the recovery mechanism by the increasing misorientation across sub-grains as the strain increases and in the dynamic recrystallization sequence by the formation of new strain free grains. In both cases areas of maximum misorientation in old grains, namely deformation bands and mantles, are favoured sites for new grain development. Most new grains appear to be related crystallographically to the old by a rotation about an *a*-axis with the range in misorientations similar to that found in deformation bands and mantles. The new and old grains have similar *c*-axes fabric patterns with the new patterns more diffuse than the old. The overall intensity of the patterns may be governed by the strain before recrystallization.

Grain growth occurs under normal tectonic conditions and may lead to new *c*-axes fabric patterns. The new grains are subjected to continuing deformation, develop optical strain features and may undergo further recrystallization. However, grain growth will be inhibited if the stress is sufficiently high to cause a rapid increase in the dislocation densities in the new grains and the result is a quartz mylonite. If the grain size is 100 μm or greater the mylonite may undergo a further cycle of deformation and recrystallization. Deformation maps indicate that a change in Coble creep may occur if the grain size is reduced to less than 100 μm, and show that the change leads to a pronounced strain softening of these mylonites and possible superplastic behaviour.

The above sequence is summarized in figure 8.

I wish to thank Dr E. H. Rutter for many beneficial discussions and for reading a draft of this manuscript, Drs C. J. L. Wilson and J. Carreras for making unpublished results available, Professors J. Sutton, F.R.S. and P. R. Swann for provision of facilities and the Royal Society for a Mr and Mrs John Jaffé Donation Research Fellowship. Figure 1 is reproduced by courtesy of *Neues Jb. Miner.*

References (White)

Ardell, A. J., Christie, J. M. & Tullis, J. A. 1973 Dislocation substructures in deformed quartz rocks. *Crystal Lattice Defects* **4**, 275–285.

Ashby, M. F. 1972 A first report of deformation mechanism maps. *Acta metall.* **20**, 887–897.

Ashby, M. F. & Verrall, R. A. 1973 Diffusion accommodated flow and superplasticity. *Acta metall.* **21**, 149–163.

Ave'Lallement, H. G. & Carter, N. L. 1971 Pressure dependence of quartz deformation lamellae orientations. *Am. J. Sci.* **270**, 218–235.

Baeta, R. D. & Ashbee, K. H. G. 1970 Mechanical deformation of quartz. *Phil. Mag.* **22**, 601–624.

Baeta, R. D. & Ashbee, K. H. G. 1973 Transmission electron microscopy studies of plastically deformed quartz. *Phys. Status Solidi* **a18**, 155–170.

Bailey, S. W., Bell, R. A. & Peng, C. J. 1958 Plastic deformation of quartz in Nature. *Bull. geol. Soc. Am.* **69**, 1443–1466.

Balk, R. 1952 Fabric of quartzites near thrust planes *J. Geol.* **60**, 415–435.

Bell, T. H. & Etheridge, M. A. 1973 Microstructures of mylonites and their descriptive terminology. *Lithos* **6**, 337–348.

Bhattacharya, D. S. & Pasayat, S. 1968 Deformation texture in quartz: A theoretical approach. *Tectonophysics* **5**, 303–314.

Cahn, R. W. 1950 Internal strains and recrystallisation. *Prog. Metal Phys.* **2**, 151–176.

Cahn, R. W. 1974 Grain boundaries in recrystallization. *Can. Met. Q.* **13**, 253–259.

Carreras, J. 1974 Progressive mylonitization in quartzitic and quartzofeldspathic rocks in shear zones. Unpublished thesis, University London.

Carter, N. L. 1971 Static deformation of silica and silicates. *J. geophys. Res.* **76**, 5514–5540.

Chin, G. Y. 1969 Tension and compression textures. In *Textures in research and practice.* Berlin: Springer. pp. 51–80.

Christie, J. M. & Ardell, A. J. 1974 Substructures of deformation lamellae in quartz. *Geology* **2**, 405–408.

Cloos, E. 1971 *Microtectonics.* Baltimore, Maryland: John Hopkins Press.

Cottrell. A. H. 1964 *Theory of crystal dislocations.* London: Gordon & Breach.

Dillamore, I. L. & Roberts, W. T. 1965 Preferred orientation in wrought and annealed metals. *Metall. Rev.* **10**, 271–380.

Dillamore, I. L. & Katoh, H. 1971 Polycrystalline plasticity and texture development in cubic metals. *Proceedings of Conference on Quantitative Texture Development.* Krakow, Poland: Inst. Akad. Gornicka Hutnicko.

Doherty, R. D. 1974 The deformed state and nucleation of recrystallization. *Met. Sci. J.* **8**, 132–142.

Fairbairn, H. W. 1950 Pressure shadows and relative movement in a shear zone. *Am. Geophys. Union Trans.* **31**, 914–916.

Fellows, R. E. 1943 Recrystallization and flowage in Appalachian quartzite. *Bull. geol. Soc. Am.* **54**, 1399–1431.

Feltham, P. & Sinclair, R. 1972 High temperature creep of copper. *Acta metall.* **20**, 1095–1099.

Frischat, G. M. 1970 Sodium diffusion in natural quartz crystals. *J. Am. Ceram. Soc.* **53**, 357.

Gifkins, R. C. 1975 A theory for creep involving grain-boundary sliding. *Acta metall.* (In the Press.)

Gordon, P. & Vandermeer, R. A. 1966 Grain-boundary migration. In *Recrystallization, grain growth and textures.* (ed. H. Margolin), Metals Park, Ohio: Am. Soc. Metals. pp. 205–266.

Hara, I., Tadeda, K. & Mimura, T. 1973 Preferred lattice orientation of quartz in shear deformation. *J. Sci., Hiroshima Univ.* c **7**, 1–11.

Hobbs, B. E. 1968 Recrystallization of single crystals of quartz. *Tectonophysics* **6**, 353–401.

Hobbs, B. E., McLaren, A. C. & Paterson, M. S. 1972 Plasticity of single crystals of synthetic quartz. *Geophys. Monogr.* **16**, 1–28.

Honeycombe, R. W. K. 1968 *The plastic deformation of metals.* London: Arnold.

Hull, D. 1965 *Introduction to dislocations.* Oxford: Pergamon.

Hutchinson, W. B. 1974 Development of textures in recrystallization. *Metal. Sci. J.* **8**, 185–196.

Johnston, M. R. W. 1961 Polymetamorphism in movement zones in the Caledonian thrust belt of north west Scotland. *J. Geol.* **69**, 417–432.

Jonas, J. J., Sellars, C. M. & Tegart, W. J. McG. 1969 Strength and structure under hot-working conditions. *Metall. Rev.* **14**, 1–24.

Kats, A. 1962 Hydrogen in alpha-quartz. *Philips Res. Rep.* **17**, 133–279.

Kirby, S. H. & Raleigh, C. B. 1973 Mechanisms of high-temperature, solid-state flow in minerals and ceramics and their bearing on creep behaviour of the mantle. *Tectonophysics* **19**, 165–194.

Lister, G. 1974 Theory of deformation fabrics. Unpublished thesis. Australian National University.

McLaren, A. C. & Retchford, J. A. 1969 Transmission electron microscope study of the dislocations in plastically deformed synthetic quartz. *Phys. Status Solidi* **33**, 657–668.

McLaren, A. C., Turner, P. G., Boland, J. N. & Hobbs, B. E. 1970 Dislocation structure of deformation lamellae in synthetic quartz. *Contrib. Mineral. and Petrol.* **29**, 104–115.

McLaren, A. C. & Hobbs, B. E. 1972 Transmission electron microscope investigation of some naturally deformed quartzites. *Geophys. Monogr.* **16**, 55–66.

McQueen, H. J. & Bergeson, S. 1972 Dynamic recrystallization of copper during hot torsion. *Met. Sci. J.* **6**, 25–29.

Marjoribanks, R. W. 1974 The structural and metamorphic geology of the Ormiston Range, Central Australia. Unpublished thesis. Australian National University.

Mohamed, F. A. & Langdon, T. G. 1974 Deformation mechanism maps based on grain size. *Met. Trans.* **5**, 2339–2345.

Nye, J. F. 1953 The flow law of ice from measurements in glacier tunnels. *Proc. R. Soc. Lond.* A **219**, 477–499.

Paterson, M. S. 1973 Nonhydrostatic thermodynamics and its geologic applications. *Rev. Geophys. Space Phys.* **11**, 355–389.

Phillips, F. C. 1945 The microfabric of the Moine Schists. *Geol. Mag.* **82**, 205–220.

Phillips, W. J. 1965 The deformation of quartz in a granite, *Geol. J.* **4**, 391–413.

Ransom, D. M. 1971 Host control of recrystallized quartz grains. *Mineralog. Mag.* **38**, 83–88.

Sah, J. P., Richardson, G. J. & Sellars, C. M. 1969 Recrystallization during hot deformation of nickel. *J. Aust. Inst. Metals.* **13**, 292–297.

Sah, J. P., Richardson, G. P. & Sellars C. M. 1974 Grain-size effects during dynamic recrystallization of nickel. *Met. Sci. J.* **8**, 325–331.

Scholz, C. 1968 Mechanism of creep in brittle rock. *J. geophys. Res.* **77**, 2104–2114.

Stocker, R. L. & Ashby, M. F. 1973 On the rheology of the upper mantle. *Rev. Geophys. Space Phys.* **11**, 391–426.

Stüwe, H. P. & Ortner, B. 1974 Recrystallization in hot working and creep. *Met. Sci. J.* **8**, 161–167.

Sutton, J. & Watson, J. 1959 Metamorphism in deep-seated zones of transcurrent movement at Kungwe Bay. *J. Geol.* **67**, 1–13.

Sylvester, A. G. & Christie, J. M. 1968 The origin of crossed-girdle orientations of optic axes in deformed quartzites. *J. Geol.* **76**, 571–580.

Tullis, J., Christie, J. M. & Griggs, D. T. 1973 Microstructures and preferred orientations of experimentally deformed quartzites. *Bull. geol. Soc. Am.* **84**, 297–314.

Twiss, R. J. 1974 Structure and significance of planar deformation features in synthetic quartz. *Geology* **2**, 329–332.

White, S. 1971*a* Natural creep deformation of quartzites. *Nature Phys. Sci.* **234**, 175–177.

White, S. 1971*b* Electrical conductivity in quartz, a reply. *Nature Phys. Sci.* **233**, 63–64.

White, S. 1973*a* The dislocation structures responsible for the optical effects in some naturally deformed quartzites. *J. Mater. Sci.* **9**, 490–499.

White, S. 1973*b* Syntectonic recrystallization and texture development in quartz. *Nature, Lond.* **244**, 276–278.

White, S. 1973*c* Deformation lamellae in naturally deformed quartz. *Nature Phys. Sci.* **245**, 26–28.

White, S. 1975 Effect of polyphase deformation on the defect structures in quartz II. *Neues Jb. Miner. Abh.* **123**, 237–252.

White, S. 1976 Estimation of strain rates from microstructural features. *Q. J. geol. Soc. Lond.* **131**, 577–583.

White, S. & Treagus, J. E. 1975 Effect of polyphase deformation on the defect structures in quartz. I. *Neues Jb. Miner. Abh.* **123**, 219–236.

Wilson, C. J. L. 1973 The prograde microfabric in a deformed quartzite sequence, Mt Isa, Australia. *Tectonophysics* **19**, 39–81.

Wilson, C. J. L. 1975 Preferred orientations in quartz ribbon mylonites. *Bull. geol. Soc. Am.* **86**, 968–974.

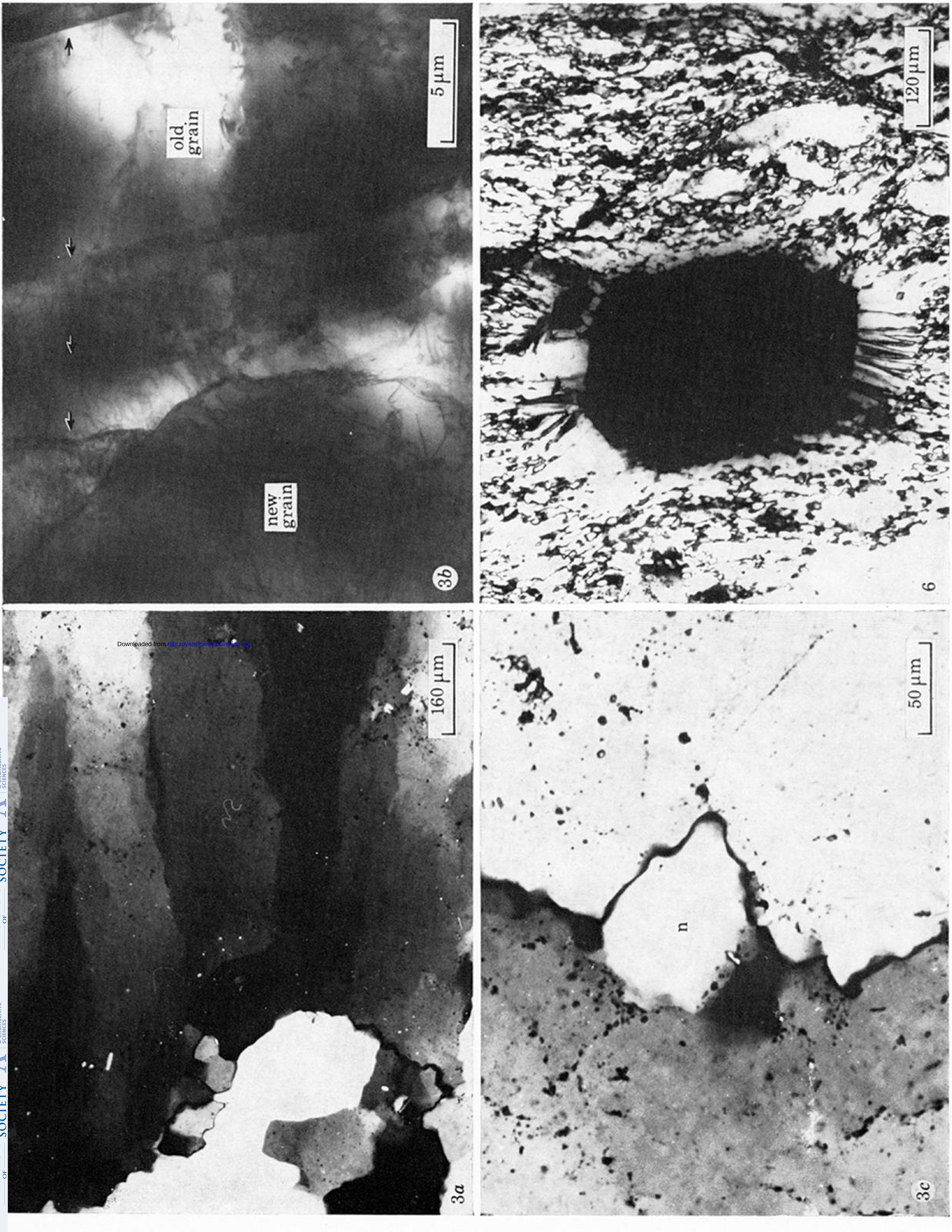

FIGURES 3 AND 6. For description see opposite.

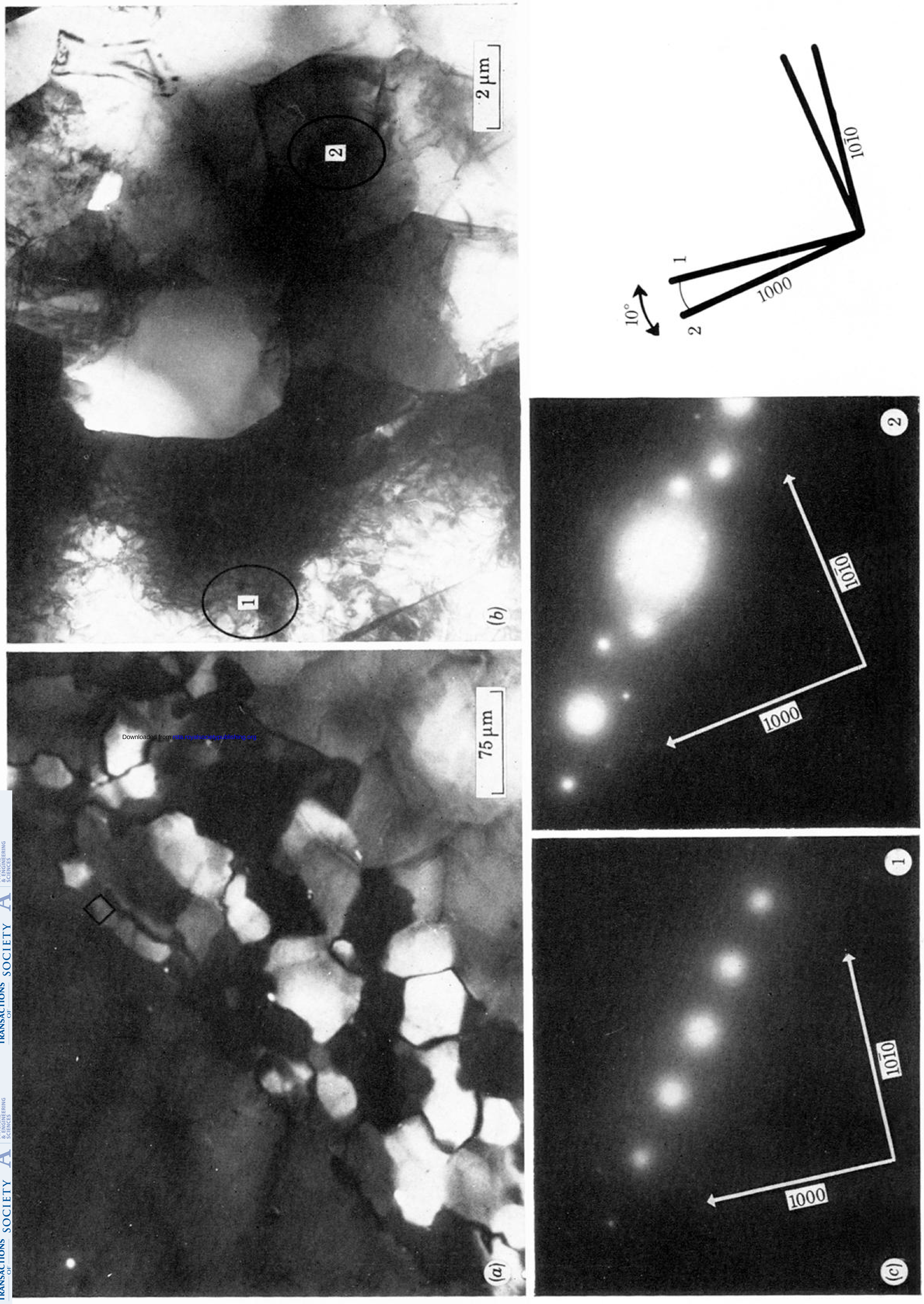

FIGURE 4. For description see opposite.